Host-Pathogen Interactions and Correlated Factors That Are Affected in Replicative-Aged *Cryptococcus neoformans*

Vanessa K.A. Silva , Sungyun Min , Kyungyoon Yoo , Bettina C. Fries *

Posted Date: 6 March 2024

doi: 10.20944/preprints202403.0330.v1

Keywords: Aging; cryptococcosis; G2 arrest; intracellular parasitism; phagosomal pH; polysaccharide capsule; vomocytosis; urease

Article

Host-Pathogen Interactions and Correlated Factors That Are Affected in Replicative-Aged *Cryptococcus neoformans*

Vanessa K.A. Silva [1], Sungyun Min [2], Kyungyoon Yoo [1] and Bettina C. Fries [1,2,3,*]

[1] Department of Microbiology and Immunology, Renaissance School of Medicine, Stony Brook University, Stony Brook, NY 11794, USA; vanessakarina.alvesdasilva@stonybrook.edu (V.K.A.S.); kyungyoon.yoo@stonybrookmedicine.edu (K.Y.)
[2] Division of Infectious Diseases, Department of Medicine, Stony Brook University, Stony Brook, NY 11794, USA; SungyunSusanne.Min@stonybrookmedicine.edu (S.M.)
[3] Veterans Administration Medical Center, Northport, NY 11768, USA; Bettina.Fries@stonybrookmedicine.edu
* Correspondence: Bettina.Fries@stonybrookmedicine.edu

Abstract: *Cryptococcus neoformans* is a facultative intracellular fungal pathogen. Ten-generation-old (10GEN) *C. neoformans* cells are more resistant to phagocytosis and killing by macrophages than younger daughter cells. However, mechanisms that mediate this resistance and intracellular parasitism are poorly understood. Here, we identified factors important for the intracellular survival of 10GEN *C. neoformans*, such as urease activity, capsule synthesis, and DNA content using flow cytometry and fluorescent microscopy techniques. Real-time visualization of time-lapse imaging was applied to determine the phagosomal acidity, membrane permeability, and vomocytosis (non-lytic exocytosis) rate in J774 macrophages that phagocytosed *C. neoformans* of different generational ages. Our results showed that old *C. neoformans* exhibited higher urease activity, and enhanced capsule formation, which was supported by an increased Golgi complex. In addition, old *C. neoformans* were more likely to be arrested in the G2 phase, resulting in the occasional formation of aberrant trimera-like cells. To finish, the advanced generational age of the yeast cells slightly reduced vomocytosis events within host cells, which might be associated with increased phagolysosomal pH and membrane permeability. Altogether our results contribute to a better understanding of the strategies used by old *C. neoformans* to resist phagosomal killing and suggest that old generation *C. neoformans* intracellular behavior may be driving cryptococcosis pathogenesis.

Keywords: aging; cryptococcosis; G2 arrest; intracellular parasitism; phagosomal pH; polysaccharide capsule; vomocytosis; urease

1. Introduction

Virulence strategies employed by the encapsulated yeast *Cryptococcus neoformans* encompass the capability to directly manipulate the host cell (Casadevall and Fang [1]. This facultative intracellular organism has adapted to reside and replicate within the acidic phagosome and escape via a non-lytic process, called vomocytosis [2]. All these mechanisms can be exploited by *C. neoformans* to transverse the lung epithelial tissues and travel in the blood circulation to disseminate as a 'Trojan horse' to extrapulmonary organs, including the brain [3].

C. neoformans is the leading cause of fungal meningitis [4]. In response to this public health threat, this fungal pathogen was recently ranked as critically important by the World Health Organization [5,6]. *C. neoformans* is a eukaryotic pathogen that undergoes asymmetric division during replication, resulting in a phenotypic dichotomy between the aging mother cell and its newly budded daughter

 doi:10.20944/preprints202403.0330.v1

[7]. Although labeled as 'old', these cells continue to exhibit fitness with unchanged doubling times, having lived only about a third of their life expectancy, and are far from senescence. *C. neoformans* cells that lived 10 generation exhibit marked resistance to phagocytic killing [8], increased melanin secretion [9], a remodeled cell wall [10] and higher tolerance to antifungals [8]. We have proposed that the persistence of cryptococcal disease and treatment failure during chronic infection is driven by the selection and accumulation of old yeast cells, which can evade the host response [8].

The arsenal of virulent factors employed by *C. neoformans* to survive inside a host cell includes the release of capsular material and the secretion of enzymes, such as urease [11,12]. For instance, the cryptococcal polysaccharide capsule [13] and unbudded cell cycle arrest [14] have been linked to loss of phagosome membrane integrity, whereas urease activity affects fitness, increases phagosomal pH within the mammalian phagosome and promotes vomocytosis [12].

Based on pivotal studies that characterized *C. neoformans* interactions with macrophages [15], we hypothesized that *C. neoformans* phagosome interaction impose selection on the *C. neoformans* population in the host. In this study, we investigated strategies used by old *C. neoformans* to thrive inside host macrophages and characterized age-associated virulence factors that contribute to fungal intracellular survival.

2. Materials and Methods

2.1. Yeast strains and isolation of old C. neoformans cells

C. neoformans wild-type strains (H99 and K99α) were maintained on YPD agar plates. Strain K99α was used for the urease activity test and H99 was used for all the remaining experiments. Yeast cells (10^8) from a six-hour exponential culture in Synthetic media (1.7 g yeast nitrogen base without amino acids, 1 g drop-out mix, 0.4% ethanol, 5 g $(NH_4)_2SO_4$, 3.3 g NaCl, 20 g glucose), at 37°C with 160 rpm shaking, were washed twice with phosphate-buffered saline (PBS) pH 7.0, and labeled with 8 mg/mL Sulfo-NHS-LC-LC-Biotin for 30 minutes at room temperature. Subsequently, *C. neoformans* cells were washed with PBS and grown 5 doubling times in the same exponential culture conditions. After, yeast cultures were washed once with PBS containing 0.5M Ethylenediaminetetraacetic acid (EDTA) for removing DNA from cell debris and reducing cell clumping, and twice with PBS. Then, 100 µL of magnetic streptavidin microbeads were added to previously labeled (10^8) cells in PBS, following incubation for 15 minutes at 4°C. Subsequently, biotin-labeled yeasts were isolated using autoMACS magnetic columns and the autoMACS Pro separator (Miltenyi Biotec). The biotin-streptavidin-labeled older cells were passed through a magnet where they got stuck, while the younger unlabeled population flew through. The labeled cells were recovered after the magnetic field was removed. The positive cell fraction was grown again in Synthetic media to the desired generation (10 GEN) and isolated as outlined above. Young cells washed off from the magnetic columns were kept as controls (adapted from [10].

2.2. Macrophage cell line culture

Cells from the murine macrophage-like cell line J774A.1 were used between passages 4 and 14 after thawing and were cultured in Dulbecco's modified Eagle's medium (DMEM) supplemented with 2 mM L-glutamine, 1% Sodium Pyruvate, 100 U/mL penicillin, 100 U/mL streptomycin and 10% fetal bovine serum (FBS) at 37°C and 5% CO_2.

2.3. Urease activity

10^7 *C. neoformans* cells were incubated in rapid urea broth (Urea 4g, Yeast extract 0.02g, Phenol Red 2 mg, KH_2PO_4 0.273g, Na_2HPO_4 0.285g, H_2O 100 ml) [16] for 3h at 37°C with agitation. Optical Density (OD) was read (λ 560 nm) and OD > 0.3 was considered as positive. Young and old *C. neoformans* cells were heat-killed for 30 minutes at 75°C [17] and were used as a negative control.

2.4. Analysis of the Golgi Apparatus

 doi:10.20944/preprints202403.0330.v1

We followed the protocol adapted for the analysis of the Golgi in cryptococci by Kmetzsch et al. (2011) and Rizzo et al. (2014). Briefly, yeast cells (10^7) were fixed with 4% paraformaldehyde in PBS, followed by washing with PBS and incubation with C6-NBD-ceramide (10 μM) for 16 h at 4°C. The cells were then incubated with fetal calf serum (10%) at 4°C for 1 h to remove the excess of C6-NBD-ceramide. The cell wall was stained with calcofluor white (5 μg/mL) for 10 min at room temperature, followed by washing with PBS and analysis by fluorescence microscopy (Nikon Eclipse 90i microscope). Different staining patterns were determined in approximately 100 cells of each strain using the ImageJ software.

2.5. Polysaccharide capsule analysis

Fungal cells (10^7) were fixed in 4% paraformaldehyde for 1 h and then incubated in PBS supplemented with 1% bovine serum albumin for 1 h at 37°C. The samples were incubated with the monoclonal antibodies (mAb) 18B7 (IgG1) at 10 μg/ml for 1 h at 37 °C [18]. After washing with PBS, the *C. neoformans* cells were incubated with an anti-murine IgG Alexa Fluor™ 488-conjugated (Invitrogen) at 10 μg/ml. Finally, the yeast cells were again washed, suspended in PBS, and analyzed by flow cytometry and fluorescent microscopy [19].

The Capsule of *C. neoformans* was analyzed on a BD LRSFortessa flow cytometer with the blue laser (488 nm). Unstained cells were used as negative controls. A total of 10,000 events were gated in the forward scatter/side scatter (FSC/SSC) plots and represented as histograms with mean fluorescence intensity (MFI) on the x-axis and cell counts on the y-axis. Data were analyzed using FlowJo v10.1 software. For fluorescence microscopy, the channels fluorescein isothiocyanate (FITC) (DyLight 488) and DAPI (4′,6-diamidino-2-phenylindole) (CFW) were used. Imaging was performed at 100× magnification in a Nikon Eclipse 90i microscope with a digital camera. The same exposure time was used to image young and old cells and the images were processed using ImageJ software.

2.6. DNA staining and cell cycle analysis

We analyzed the DNA levels and cell cycle by staining *C. neoformans* cells with propidium iodide according to previous study [20]. Briefly, after standard magnetic bead-based isolation, $5x10^6$ cells of (young and old) *C. neoformans* H99 and diploid strain #K24 cells (positive control) were centrifugated at 500 RCF for 3 minutes and then fixed with 500 μl of 70% ethanol overnight at 4°C with rotation. The next day, the cells were centrifuged again at 500 RCF for 3 minutes, and pellets were washed once in 500 μl of 50 mM sodium citrate. The cell suspensions were sonicated for 10-15 seconds at 30% power. The sonicated cells were centrifuged again at 500 RCF for 3 minutes, and the supernatants were gently aspirated and resuspended in 200 μl of 20 mM sodium citrate with 0.5 mg/ml RNAse, and gently mixed. The samples were incubated at 37°C for 2-4h with rotation. Subsequently, 10 μl aliquots of each suspension were reserved to be used as unstained cells (negative control), and 5 μl of 50 mM sodium citrate and 5 μl of Propidium iodide (PI, 1 mg/ml) were added to the rest of the cell suspensions, resulting in a final concentration of 25 μg/ml per sample. Following incubation overnight in the dark at 37°C with rotation, the samples were sonicated for 5-10 seconds at 15% of total power and immediately before analyzing on the flow cytometer to dissociate any cell clumps. To avoid dye leaching out of the cells, the samples were diluted 1/40 into the PI buffer (25 μg/ml PI in 50 mM sodium citrate). To ensure statistical power in the analysis, at least 20,000 events per sample were acquired using a BD LRSFortessa flow cytometer with the blue laser (488 nm) and the PE channel.

2.7. Phagocytosis assay, phagosomal acidification, and phagosomal permeability

J774A.1 macrophages (10^5 cells/well) were seeded into a 24-well plate for 18h, following activation with phorbol 12-myristate 13-acetate (PMA) (15 ng/mL) for 1h. As controls, yeasts (2.5 x 10^6 cells) were heat-killed at 60°C for 1h before opsonization with 10% human serum [21].

To analyze the pH alterations in the phagosomes infected with young and old *C. neoformans*, we used the amine-reactive pH-dye Phrodo green^{AM} (P35373, Thermo Fisher Scientific) to label the

 doi:10.20944/preprints202403.0330.v1

surface of *C. neoformans*, according to the manufacturer's instructions and adapted from [15,22]. This staining is non-fluorescent at neutral pH but becomes fluorescent at acidic pH. *C. neoformans* young and old cells (2.5 x 10^6 cells) were labeled with 500 µL of a solution containing 5 µl of pHrodo staining, 50 µl of Power load concentrate, and 5 mL of PBS. The yeast cells were incubated in the dark for 30 minutes at 37°C with rotation. After, yeast cells were pelleted as resuspended in DMEM supplemented with 2 mM L-glutamine, 1% Sodium Pyruvate, 100 U/mL penicillin, 100 U/mL streptomycin. Macrophages were then infected for 2 hours with serum-opsonized *C. neoformans* (MOI 10:1) at 37°C and 5% CO_2. After phagocytosis, wells were washed with PBS, at least three times, to remove extracellular *C. neoformans*. Based on previous evidence, the phagosomal acidification behaviors in *C. neoformans* were classified as 1. Acidic, 2. Delayed acidification, and 3. non-acidic [15,21].

Alternatively, two hours post-infection, the medium was replaced with serum-free DMEM supplemented with 50 nM LysoTracker® Red DND-99 to check on phagosomal permeability. Yeast cells were then taken for time-lapse microscopy as described [15,21].

2.8. Time-lapse microscopy and vomocytosis rate

Time-lapse movies were made using a Nikon Ti2-E PFS with Live-Cell Imaging with Tokai Hit Enclosure Incubator with Gas Mixing. Samples were incubated at 37°C and 5% CO2 in the microscope imaging chamber. Images were taken every 5 min for 2 hours and compiled into single movie files for analysis using NIS Elements or ImageJ software, respectively. Movies were blinded by a third party before manual scoring for vomocytosis and phagosome acidity. Macrophages infected with *C. neoformans* containing at least one acidic phagolysosome were counted as acidic. Vomocytosis was scored visually using the following previously established guidelines [2]: (a) One vomocytosis event is the expulsion of internalized cryptococci from an infected macrophage, regardless of the number of cryptococci expelled if they do so simultaneously; (b) Vomocytosis events are scored as independent phenomena if they occur in different frames or from different macrophages; (c) Vomocytosis events are discounted if the host macrophage subsequently undergoes lysis or apoptosis within 30 min.

2.9. Data analysis

All experiments were done in biological triplicates otherwise stated. Data were plotted using GraphPad Prism and statistically analyzed by comparing young and old groups, using a *t*-test with post-Welch corrections. Images and videos were processed using ImageJ or the NIS-Elements Viewer software. Flow cytometry data were analyzed using the FlowJo software, and doublets were excluded using the following gating strategy of creating a scatterplot of PI (area) by PI (width). Single cells fell in a vertical line along the PI (width) axis. Cells were then gated to exclude auto-fluorescence using unstained control cells. Cell cycle analyses were performed using the Dean-Jet-Fox algorithm.

3. Results

3.1. Effects of aging on urease activity in C. neoformans

Urease-mediated ammonia can neutralize acidic microenvironments, helping pathogens to survive hostile pH of the phagolysosome [12]. We therefore tested if old C. neoformans produce more urease than young cells. For this, we analyzed the urease activity of young and old C. neoformans. The quantification of urease activity of old C. neoformans showed remarkable increase in comparison to young C. neoformans ($p < 0.001$) (Figure 1).

 doi:10.20944/preprints202403.0330.v1

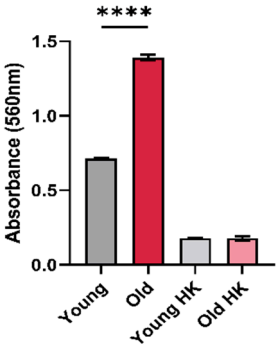

Figure 1. Urease activity in young and old *C. neoformans*. Urease enzymatic activity levels are up in old *C. neoformans* cells in comparison with young *C. neoformans* (****, $p < 0.001$). Yeast cells were incubated at rapid urea broth for 3h at 37°C with agitation and optical Density (OD) was read (λ 560 nm). OD > 0.3 was considered positive and heat-killed (HK) cells were was used as a negative control. The graph represents one biological triplicates of three independent experiments with similar results.

This suggests that old C. neoformans exhibit superior abilities to hydrolyze urease activities than young C. neoformans.

3.2. Longevity in C. neoformans affects Golgi apparatus and capsular GXM

Since the expression of the polysaccharide capsule can also affect the fate of the yeast within the host cell [11], we next investigated the impact of genrational age on GXM synthesis, the major cryptococcal capsule polysaccharide. Prior quantitative analysis by immunogold labeling had detected siginificant increase of intracellular GXM associated with vesicular structures, vacuoles and in the cell wall in old compared to young C. neoformans cells [10]. Since GXM is synthesized in the Golgi complex [23], we used the Golgi marker N-[7-(4-nitrobenzo-2-oxa-1, 3-diazole)]-6-aminocaproyl-D-erythro-sphingosine (C6-NBD-ceramide) to evaluate the morphological aspects and distribution of the Golgi apparatus in young and old C. neoformans (Figure 2A). The peripherical pattern was predominant both in young (66.85%) and old (60%) C. neoformans (Table 1). However, in old C. neoformans Golgi staining was significantly more intense compared to that in young cells (MFI levels: 5184.91 vs. 8115.95) (Figure 2B). These results suggested an increase in the size of the Golgi apparatus in C. neoformans cells of advanced generational age.

Next, we compared staining patterns of the polysaccharide capsule by fluorescent microscopy and flow cytometry after staining with the GXM-specific monoclonal antibody 18B7. Although antibody binding patterns on the capsule architecture were similar in young and old C. neoformans (Figure 3A), the quantitative levels of capsular GXM were significantly higher in old compared to young C. neoformans cells (**, p=0.0082) (Figure 3B). These data suggest that old C. neoformans produce and anchor more GXM on the capsule than young cells.

Table 1. Golgi morphologies pattern in young and old *C. neoformans*.

Golgi Morphology	Young	Old
Peripherical	62.85%	60%
Central	37.15%	40%

Preprints.org (www.preprints.org) | NOT PEER-REVIEWED | Posted: 6 March 2024 doi:10.20944/preprints202403.0330.v1

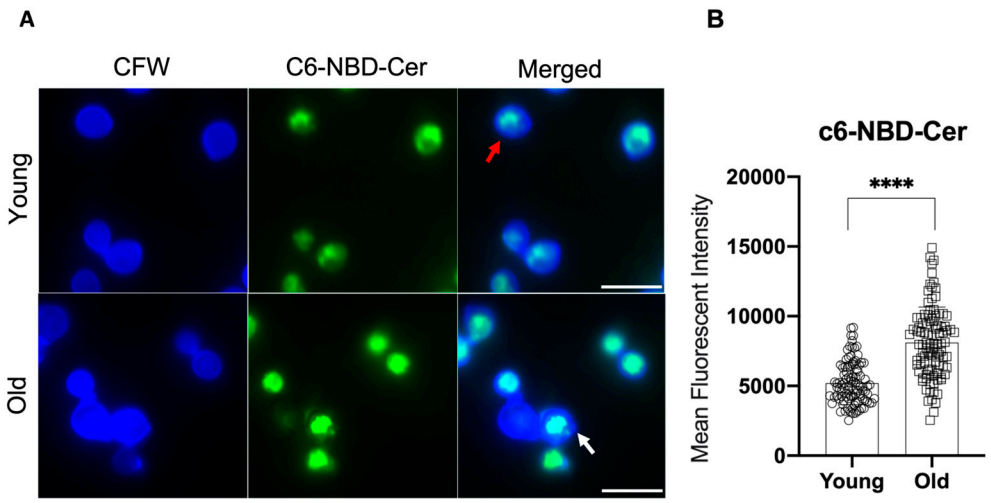

Figure 2. Influence of replicative aging of *C. neoformans* in the Golgi apparatus morphological aspects. (A) Young (Y) and old (O) *C. neoformans* cells were labeled with C6-NBD-ceramide (green) and the cell wall was stained with calcofluor white (blue). Peripherical (red) or central (white) Golgi morphologies are indicated by the arrows. Scale bars represent 10 μm. Images were taken using a fluorescent microscope at 100x and analyzed using Image J software. (B) Quantitative analysis of the morphological profiles that predominated in young and old yeast cells. At least 100 cells per group were analyzed and statistical analyzes were performed using unpaired t-test with post-Welch's correction (**** $p < 0.0001$).

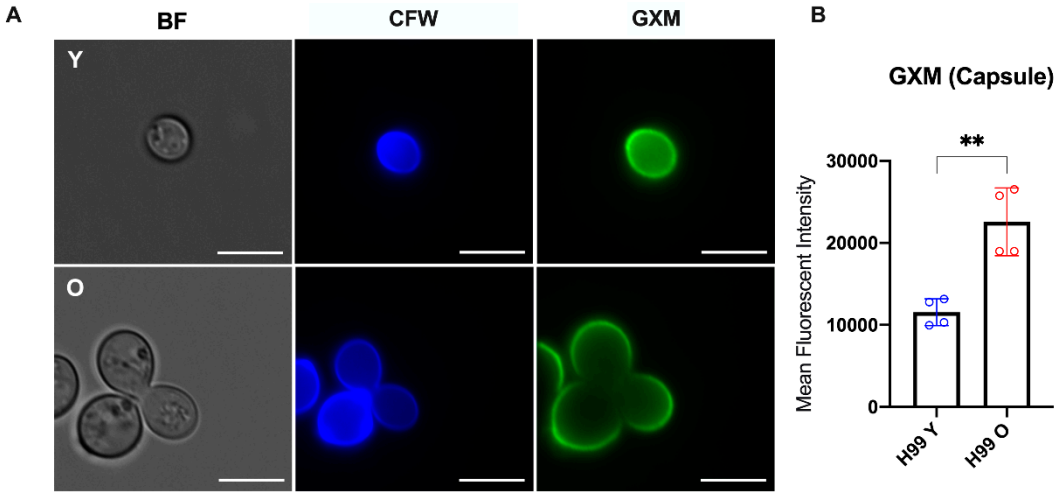

Figure 3. Morphological capsule analysis of *C. neoformans*. (A) Representative images of young (Y) and old (O) yeast cells observed by fluorescence microscopy (GXM: green; Cell wall chitin: blue). Stained cells were imaged using a fluorescent microscope at 100 x magnification and the following channels: DAPI (CFW, calcofluor white and GFP (GXM, 18B7-IgG Alexa Fluor 488), BF (brightfield). The scales bar represents 10 μm. (B) Flow cytometry to quantify the capsular GXM levels showed significantly higher amounts of capsular GXM for old (red) than young (blue) *C. neoformans* (**, $p < 0.001$). Statistical analysis was performed by t-test with Welch's correction from two biological replicates.

3.3. Old C. neoformans presented an increase in DNA content and G2 arrest

Prolonged cell cycle progression leads to C. neoformans cell with larger capsules, which was also associated with reduced phagocytosis and enhanced intracellular survival [24]. Since old C. neoformans exhibited increased binding of polysaccharide mAb 18B7, impaired phagocytosis and

 doi:10.20944/preprints202403.0330.v1

enhanced intracellular survival [7–9], we investigated if old C. neoformans cells had altered DNA content indicative of a specific cell cycle state.

To determine the DNA content of young and old C. neoformans, yeast cells were fixed, stained with PI, and examined using fluorescence flow cytometry. DNA levels were estimated based on fluorescence intensity. These data demonstrated a statistically significant overall increase in nuclear fluorescence intensity in old C. neoformans cells when compared to young C. neoformans (Figure 4A, $p < 0.05$). This increase in the DNA content was consistent with a prolongation in the G2 phase in old C. neoformans (Figure 4B, $p < 0.001$). However, no change in fungal ploidy was observed for both of the groups (Figure 7C).

In addition, we hypothesized the formation of unbudded cells of old C. neoformans as a consequence of the delayed G2 phase. Indeed, only old-generation C. neoformans produced ooccasional yeast cells with morphological abnormalities, including cells of ellipsoidal shape, resembling a trimera yeast cell with two daughter cells formed from the same mother cell, or containing a granddaughter grown from the daughter cell (Figure 4D). These unusual tubular structures would suggest aberrant mitosis following the unbudded G2 arrest and reentry into the cell cycle. Taken together, these data indicate that aging has an effect on DNA quantity and cell cycle, leading to delay in a prolonged G2 phase with morphological abnormalities such as trimera-like cell morphology.

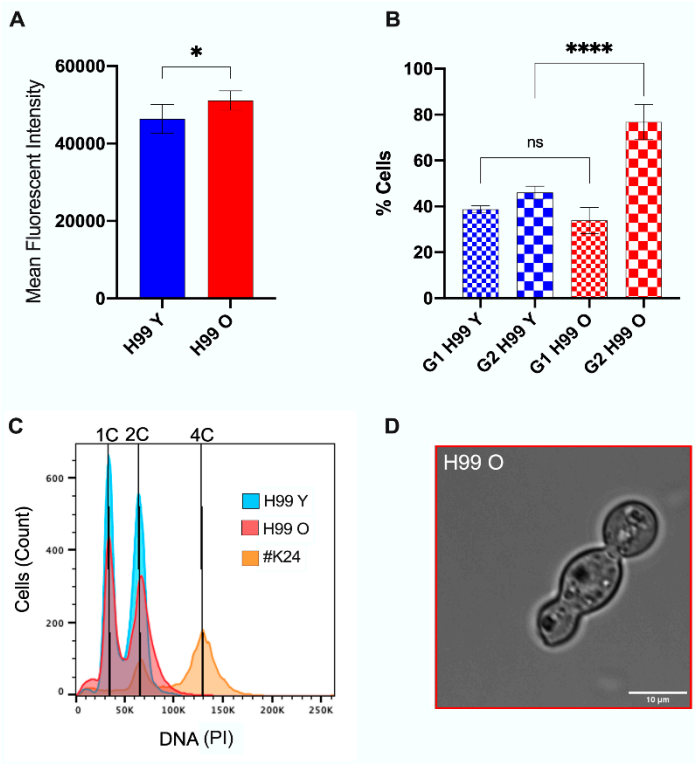

Figure 4. Old generation *C. neoformans* cells presented G2 arrest. (A) *C. neoformans* cells were fixed, stained with propidium iodide, and analyzed by flow cytometry for DNA content levels of young (blue) and old (red) *C. neoformans*. (B) Percentages of G1 and G2 phases in *C. neoformans* young (blue) and old (red) yeast cells. Unpaired t-test with Welch's correction was performed to compare young and the old groups (* $p < 0.01$, **** $p < 0.0001$, and ns: nonsignificant $p = 0.2908$). (C) Representative histograms to determine cell ploidies within the population showing peaks for *C. neoformans* cells of wild-type strain young (H99 Y) in blue, old in red (H99 O), and control diploid *C. neoformans* strain (#K24) in orange. (D) Brightfield image of the atypical elongated old *C. neoformans* cell, resembling trimera-like formation.

 doi:10.20944/preprints202403.0330.v1

3.4. Vomocytosis phenomenon during replicative aging in C. neoformans

Vomocytosis is a morphologically and temporally diverse process that occurs during macrophage infection [25]. We further explored the fate of young and old C. neoformans cells in the course of macrophage interactions with regard to vomocytosis (Figure 5A, Movie S1). Vomocytosis can be classified as type I (complete emptying of macrophage) or II (partial emptying of macrophage) [25]. Although vomycytosis was a rare outcome, macrophages infected with young C. neoformans experienced a higher rate of vomocytosis events compared to macrophages infected with old C. neoformans (Figure 5B). All vomocytosis events for macrophages infected with old C. neoformans were type I, whereas the 55% of vomocytosis events involving young C. neoformans ingested by macrophages were type II and 45% were type I. All vomocytosis events observed for both groups were in non-acidic macrophages. These results indicate that younger C. neoformans cells are more likely to undergo non-lytic expulsion than old C. neoformans, and interstingly more than half of the non-lytic expulsions of young yeast cells were incomplete.

Escape by macrophages can be influenced by phagolysosomal pH [26]. Thus, we further analyzed acidification of the host macrophages infected with young and old C. neoformans.

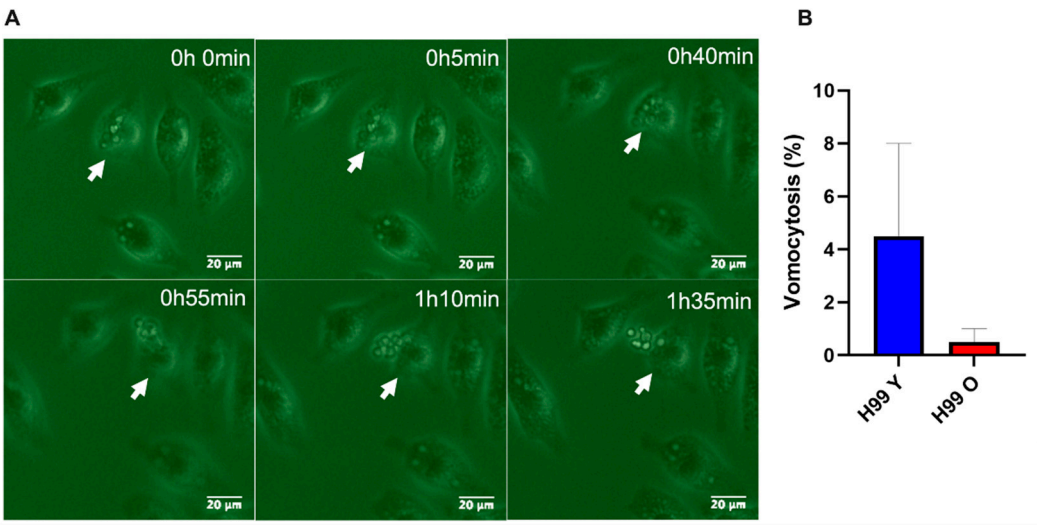

Figure 5. Vomocytosis events in macrophages (J774.A1) infected with young (Y) and old (O) *C. neoformans*. (A) Representative real-time imaging of vomocytosis type II event (white arrow) for macrophages infected with young *C. neoformans*. (B) Time-lapse microscopy videos were manually scored for the vomocytosis of *C. neoformans* from at least 100 macrophages containing yeast cells for each group until two hours after the phagocytosis assay. The graph shows the percentage of *C. neoformans*-infected macrophages which have experienced at least one vomocytosis event. Data from two independent experiments is shown. Categorical vomocytosis data were analyzed by t-test followed by Welch's correction ($p = 0.455$).

3.5. Old C. neoformans prefer to reside in acidified phagosomes

Acidification is indicative of phagosomal maturation and variations on the phagosomal acidic levels have been observed among macrophages infected with C. neoformans [15]. Here, we analyzed three distinct phagolysosomal response patterns: acidified phagolysomes (behaviour 1), delayed acidification (behaviour 2), and no acidification (behaviour 3). For macrophages containing young C. neoformans, the most commonly (61%) observed behavior was absence of acidification (behaviour 3). Whereas rapid acidification was sustained up to 120min (behaviour 1) was found in 38% of macrophages infected with young cells. In contrast, only 43% of the macrophages containing old C. neoformans exhibited no acidification of phagolysosomes (behavior 3) whereas more than half (55%) had acidified phagolysosomes for up 120 min (behaviour 1). Delayed acidification was uncommon both after phagocytosis of young (2%) and old (1%) C. neoformans. (Figure 6A an B). As expected, control experiments with heat-killed young or old C. neoformans confirmed that live fungus was

 doi:10.20944/preprints202403.0330.v1

required to modulate the phagolysosomal pH [27] (Figure 6C). When the mean fluorescence intensity (MFI) of only acidic phagosomes infected with either young or old C. neoformans was compared, MFI levels were found to be significantly higher for phagosomes containing young C. neoformans ($p < 0.001$, Figure 6D) consistent with a lower phagolysosomal pH. It is noteworthy that this difference was not caused by variations in the number of yeast cells per macrophage (Figure 6E). Taken together, these results indicate that although phagocytosis of old C. neoformans are more likely to lead to acidified phagolysosomes, the acidification is less pronounced than that of phagolysosomes containing young C. neoformans. The higher percentage of non-acidified phagolysosomes in macrophages infected with young C. neoformans was also associated with higher number of vomocytosis events which also included incomplete expulsion.

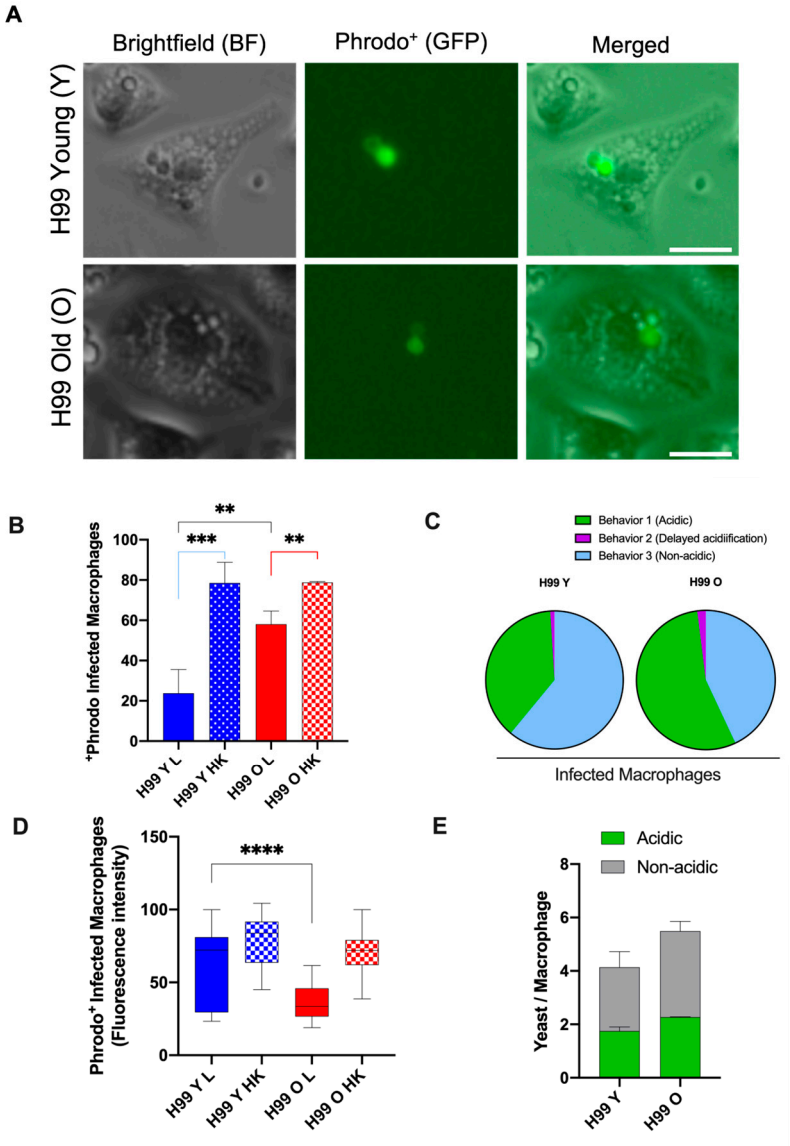

Figure 6. Effect of replicative aging on phagosomal maturation in macrophages containing *C. neoformans*. (A) Represented image of fluorescent microscopy of macrophage mouse cell line J774.A1 infected with previously pHrodo-labeled cryptococci young and old (MOI of 10) after phagocytosis, showing acidified phagosomes. Scale bar represents 20 µm. (B) Macrophages were cultured with pHrodo-labeled live (L) cryptococci (young or old) or given the respective heat-killed (HK) yeast cells (positive control). Time-lapse microscopy videos of two hours post phagocytosis were manually scored for the percent change in pHrodo$^+$ macrophages. At least 100 infected macrophages for each group were observed and statistical analysis of two independent experiments was performed by *t*-test followed by post-Welch's correction. The black line represents comparisons between young and

 doi:10.20944/preprints202403.0330.v1

old *C. neoformans*, the blue line between live and HK young *C. neoformans*, and the red line between live and HK old *C. neoformans* (** p< 0.01, *** p < 0.001). (C) Quantification of all behaviors of J774.A1 cells infected with *C. neoformans* (young and old) for up to two hours after phagocytosis (D) Quantification of Phrodo^{+} fluorescence intensity of macrophages ingested with either young (blue) or old (red), and their respective HK yeast cells (positive control). Images of at least 100 infected macrophages for each group were analyzed using ImageJ. Statistical analysis of two independent experiments was done using an unpaired *t*-test and with post-Welch's correction to compare macrophages ingested with live young against live old *C. neoformans* (**** p < 0.0001). (E) Quantification of the number of yeast *C. neoformans* cells per acidic (Phrodo^{+}, green) or non-acidic (Phrodo^{-}, gray) macrophages. At least 100 macrophages infected with young (H99 Y) or old (H99 O) *C. neoformans* were analyzed. Comparison between groups of two independent experiments was performed by unpaired *t*-test and post-Welch's correction (p = 0.2715).

3.2. Generational age in C. neoformans influences lysosomal permeabilization

We next analyzed the phagosome leakage because C. neoformans *can manipulate phagosome acidification by permeabilizing the phagosome membrane* [15]. Lysosome damage is crucial for intracellular C. neoformans survival strategy and contributes to fungal virulence [28]. Therefore, we assessed phagolysosomal permeabilization by real-time visualization and measuring LysoTracker DeepRed intensity, which localizes to this acidic organelle [12]. The number of cells presenting loss of Lysotracker fluorescence was quantified after 2h of infection. Macrophages infected with old C. neoformans developed significantly reduced Lysotracker fluorescence, indicating phagolysosomal membrane permeabilization. In contrast, macrophages infected with young C. neoformans retained higher levels of the lysotracker fluorescence (Figure 7), suggesting the maintenance of phagolysosomal membrane integrity. As expected the analysis of macrophages infected with heat-killed C. neoformans manifested no loss of fluorescence signal.–

We synthesized the observations of this study in Figure 8.

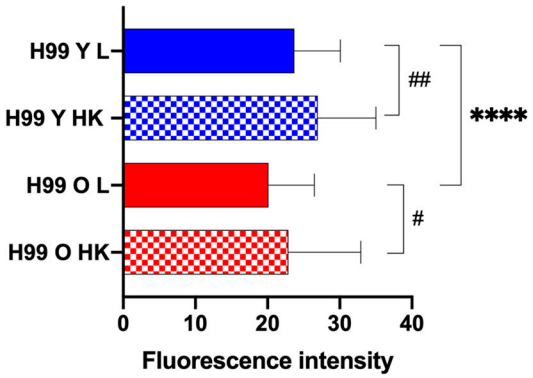

Figure 7. Phagosomal permeability of macrophages infected with *C. neoformans*. The frequency of phagosomal membrane permeability of macrophages infected with live (L) young (H99 Y, blue) and old (H99 O, red) *C. neoformans* and, respective heat-killed (HK) controls, were measured using Lysotracker deep red staining. Macrophages with permeable phagosomes were determined by loss of Lysotracker deep red. The data shown is the quantification of loss of the staining intensity verified in 100 infected macrophages, for each group, using images acquired after two hours of infection. Images were taken using Nikon Ti2-E PFS and analyzed by ImageJ. The bar chart shows the comparison of macrophages containing young with old *C. neoformans* (asterisk symbols) and live with HK *C. neoformans* (hashtag symbols). P values by t-test with Welch's correction (**** p < 0.001, # p <0.05, ## p < 0.01). .

 doi:10.20944/preprints202403.0330.v1

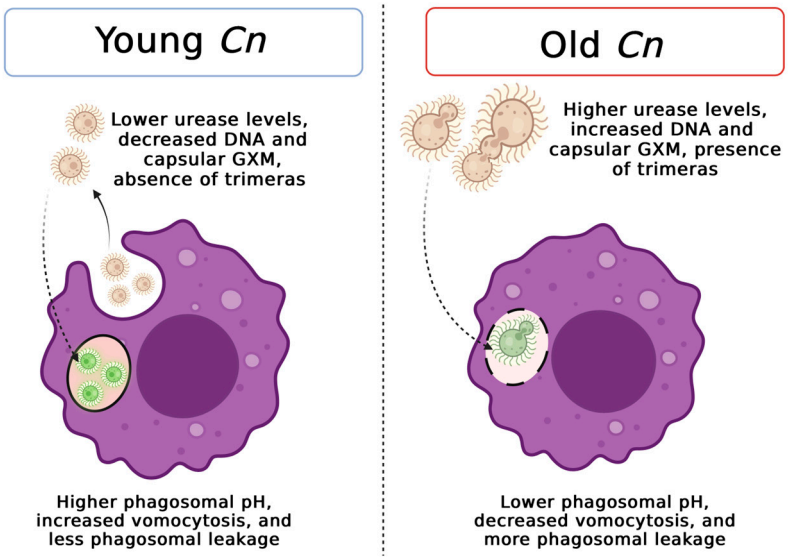

Figure 8. Schematic representation of replicative aging effects on the interactions of young and old *C. neoformans* (*Cn*) with host macrophage cells and fungal virulence-associated factors with intracellular persistence. This illustration was created using Biorender.

4. Discussion

Interactions with macrophages play a crucial role during *C. neoformans* infection [29]. Phagosomal maturation involves fusion with lysosome with subsequent acidification. This process is determined by phagosomal cargo and is critical for the activation of mechanisms associated with antigen processing and presentation [30]. The survival of intracellular cryptococci despite the acidic luminal pH involves multiple antioxidant tools such as expression of enzymes, pigment production [31], and production of capsular polysaccharide [27].

Previously, our lab showed that ten-generation old *C. neoformans* cells are significantly more resistant to killing by macrophages than their daughter cells [8,32]. However, major selection pressure would have to be operative to privilege these relatively rare old *C. neoformans* cells in the host environment. Accumulation of yeast cells with advanced generational age has been documented both for *C. neoformans* and *Candida glabrata* in several infection models [33]. Advanced generational age of *C. neoformans* cells is associated with increased melanin synthesis, reduced phagocytosis, and a thicker cell wall when compared to daughter cells [8,32]. Here we report that old *C. neoformans* produce increased levels of urease and capsular GXM, as well as higher DNA content than young yeast cells.

Urease activity leads to ammonia production and elevation of phagosomal pH since phagosomes containing *C. neoformans* (*ure1Δ*) lacking urease activity presented increased pH when compared to macrophages loaded with the wild-type strain [12]. In association with this finding, previous report has shown that increasing the phagosomal pH with chloroquine is related to enhanced antifungal activity in macrophages infected with *C. neoformans* [34]. Our comparative analysis of phagosomal pH is compelling because although a higher percentage of macrophages exhibit acidic phagosomes after ingesting old *C. neoformans* cells compared to those that phagocytose young *C. neoformans*, the pH of the acidic phagolysosomes is significantly lower when loaded with young *C. neoformans* (as shown in Figure 6B and D). These data are consistent with published studies [15], which have shown that *C. neoformans* opposed to other phagocytosed yeasts has the unique ability to manipulate the acidification of their phagosomes. Studies with mutants have supported this concept that specific cryptococcal virulence factors such as polysaccharide capsule, and urease determine phagosomal dynamics. It is possible that augmented excretion of urease into the phagolysosome by old *C. neoformans* leads to the higher phagosomal pH. Additionally, the finding that old cells produce more polysaccharides may enhance the ability of ingested *C. neoformans* to

 doi:10.20944/preprints202403.0330.v1

better buffer phagosomal acidification [13]. Expansion of the Golgi apparatus, and presence of GXM in vesicles in old *C. neoformans* are consistent with the production of more polysaccharide and the expression of an enlarged polysaccharide-capsule.–

Lower pH was also associated with better *C. neoformans* replication [12]. Whether differences in phagosomal pH result is altered intracellular replication rates cannot be determined with the current experimental design, which only imaged up to 120 minutes. This technical limitation is because old *C. neoformans* would start replicating and generate a mixed population of younger daughter cells and older mother cells, which would make it difficult to differentiate the impact of aging. For the same reason we did not assess intracellular replication rates.

Our data demonstrates decreased lysotracker fluorescence in macrophages infected with old *C. neoformans*. Loss of acidity in phagosome could also be the result of enhanced phagosomal membrane leakage, which was documented in macrophages two hours after phagocytosis of old yeast cells. The accumulation of infected macrophages with *C. neoformans* has been shown to lead to rupture of the phagocytic cell [35]. Furthermore, the physical stress on membranes from capsular enlargement has been also linked to phagosomal leakage [13]. We have shown that aging results in GXM-containing vesicles [10], cell and capsule enlargement [7] all of which could be related to both the more pronounced loss of acidity as well as loss in phagosomal integrity in old cells.

Furthermore, unbudded G2 arrest has been associated with changes in *C. neoformans* morphology, such as hyphal formation [36]. We observed trimera-like old *C. neoformans* cells, most likely because aging promotes G2 arrest. Since cell cycle arrest is also an important stress response mechanism in the murine pulmonary environment [14], we hypothesized that these alterations in the morphology of old cells could also contribute to phagosomal integrity, resistance to phagocytic killing and even favor the rupture of the host phagocytic cells. Interestingly, *C. albicans* exposed to fluconazole forms three-lobed trimeras. These trimeras produce genetically variable progeny with varying numbers of chromosomes, increasing the odds of creating a drug-resistant strain (REF). Our analysis by flow cytometry for DNA content of propidium iodide-stained cells is likely not sensitive enough to identify aneuploidies. Also, old *C. neoformans* were not grown and isolated in the presence of fluconazole selection pressure [37].

Lastly, phagosome membrane permeabilization in macrophages infected with *C. neoformans* has been associated with a decrease in vomocytosis events [13], as well as higher intracellular pH [22]. Non-lytic expulsion can be facilitated from non-acidic phagosomes [38], which explains why we find more vomocytosis in macrophages that phagocytosed young C. *neoformans* cells, as they have a significantly higher percentage of non-acidified phagosomes. Longer live-imaging videos would likely have captured more vomocytosis events, majority of *C. neoformans* are reported to exit via non lytic expulsion after six hours [25]. Prolonged imaging and analysis of more infected phagocytic cells would also clarify if dragatocytosis (lateral transfer from one macrophage to subjacent macrophage) is enhanced in macrophages infected with old *C. neoformans*. Previous studies have demonstrated that the actin flash formation may be a macrophage mechanism to avoid *C. neoformans* escape by vomocytosis [22]. Given that the size, capsule, and cell wall is markedly altered in old *C. neoformans* it is conceivable that the actin flash formation also differs in macrophages infected with old *C. neoformans* when compared to young *C. neoformans*.

Taken together, our data suggest that aging of *C. neoformans* results in altered interactions with the phagolysosomes in macrophages, which supports our hypothesis that macrophages play a key role in the selection process of old *C. neoformans* during infection. Old *C. neoformans* prevail within acidic phagolysosomes and manipulate the phagosomal pH, both of which is consistent with their enhanced resistance to macrophage killing. Future experiments employing prolonged live imaging studies and aged urease and capsular mutants will help to further elucidate the effect of old *C. neoformans* on phagosomal interactions and intracellular fate. The comprehension of these essential host-pathogen interactions could further shed light on mechanisms that bring new insights for novel antifungal therapeutic design.

Supplementary Materials: The following supporting information can be downloaded at the website of this paper posted on Preprints.org.

Author Contributions: V.K.A.S. contributed significantly to the study design. Conceptualization, V.K.A.S. and B.C.F.; methodology, V.K.A.S. and K.Y.; formal analysis, V.K.A.S., K.Y., and S.M.; investigation, V.K.A.S. and B.C.F.; resources, B.C.F.; writing—original draft preparation, V.K.A.S.; writing—review and editing, V.K.A.S. and B.C.F..; supervision, B.C.F.; project administration, B.C.F.; funding acquisition, B. C. F. All authors have read and agreed to the published version of the manuscript.

Funding: This research was funded by the National Institutes of Health (NIH 1R01AI127704- 01A1 to B.C.F.). B.C.F. is attending at the U.S. Department of Veterans Affairs-Northport VA Medical Center, Northport, NY. She is supported by US Veterans Affairs Merit Review Award 5I01 BX003741 and NIAID R R56AI127704-06A1. The contents of this review do not represent the views of VA or the United States government.

Institutional Review Board Statement: Not applicable.

Informed Consent Statement: Not applicable.

Data Availability Statement: All data required to understand this article are presented in the study. Any raw data further requests will be provided by the corresponding authors.

Acknowledgments: We thank the Flow Cytometry Research Core Facility at Stony Brook Hospital. We are also thankful to Dr. Agnieszka B. Bialkowska and Dr. Sian Piret for allowing us to use the fluorescent microscope. MAb 18b7 was a gift from Dr. Arturo Casadevall and the diploid strain (#K24) was a donation from Dr. Joseph Heitman.

Conflicts of Interest: The authors declare no conflict of interest.

References

1. Casadevall, A.; Fang, F.C. The intracellular pathogen concept. *Molecular Microbiology* **2020**, *113*, 541-545, doi:https://doi.org/10.1111/mmi.14421.
2. Gilbert, A.S.; Seoane, P.I.; Sephton-Clark, P.; Bojarczuk, A.; Hotham, R.; Giurisato, E.; Sarhan, A.R.; Hillen, A.; Velde, G.V.; Gray, N.S.; et al. Vomocytosis of live pathogens from macrophages is regulated by the atypical MAP kinase ERK5. *Sci Adv* **2017**, *3*, e1700898, doi:10.1126/sciadv.1700898.
3. Chen, Y.; Shi, Z.W.; Strickland, A.B.; Shi, M. Cryptococcus neoformans Infection in the Central Nervous System: The Battle between Host and Pathogen. *Journal of Fungi* **2022**, *8*, 1069.
4. Rajasingham, R.; Smith, R.M.; Park, B.J.; Jarvis, J.N.; Govender, N.P.; Chiller, T.M.; Denning, D.W.; Loyse, A.; Boulware, D.R. Global burden of disease of HIV-associated cryptococcal meningitis: an updated analysis. *The Lancet Infectious Diseases* **2017**, *17*, 873-881, doi:https://doi.org/10.1016/S1473-3099(17)30243-8.
5. Rodrigues, M.L.; Nosanchuk, J.D. Recognition of fungal priority pathogens: What next? *PLoS Negl Trop Dis* **2023**, *17*, e0011136, doi:10.1371/journal.pntd.0011136.
6. Fisher, M.C.; Denning, D.W. The WHO fungal priority pathogens list as a game-changer. *Nat Rev Microbiol* **2023**, *21*, 211-212, doi:10.1038/s41579-023-00861-x.
7. Jain, N.; Cook, E.; Xess, I.; Hasan, F.; Fries, D.; Fries, B.C. Isolation and Characterization of Senescent Cryptococcus neoformans and Implications for Phenotypic Switching and Pathogenesis in Chronic Cryptococcosis. *Eukaryotic Cell* **2009**, *8*, 858-866, doi:doi:10.1128/ec.00017-09.
8. Bouklas, T.; Pechuan, X.; Goldman, D.L.; Edelman, B.; Bergman, A.; Fries, B.C. Old Cryptococcus neoformans Cells Contribute to Virulence in Chronic Cryptococcosis. *mBio* **2013**, *4*, 10.1128/mbio.00455-00413, doi:doi:10.1128/mbio.00455-13.
9. Orner, E.P.; Zhang, P.; Jo, M.C.; Bhattacharya, S.; Qin, L.; Fries, B.C. High-Throughput Yeast Aging Analysis for Cryptococcus (HYAAC) microfluidic device streamlines aging studies in Cryptococcus neoformans. *Communications Biology* **2019**, *2*, 256, doi:10.1038/s42003-019-0504-5.
10. Silva, V.K.A.; Bhattacharya, S.; Oliveira, N.K.; Savitt, A.G.; Zamith-Miranda, D.; Nosanchuk, J.D.; Fries, B.C. Replicative Aging Remodels the Cell Wall and Is Associated with Increased Intracellular Trafficking in Human Pathogenic Yeasts. *mBio* **2021**, *13*, e0019022, doi:10.1128/mbio.00190-22.
11. Alvarez, M.; Casadevall, A. Phagosome extrusion and host-cell survival after Cryptococcus neoformans phagocytosis by macrophages. *Curr Biol* **2006**, *16*, 2161-2165, doi:10.1016/j.cub.2006.09.061.
12. Fu, M.S.; Coelho, C.; De Leon-Rodriguez, C.M.; Rossi, D.C.P.; Camacho, E.; Jung, E.H.; Kulkarni, M.; Casadevall, A. Cryptococcus neoformans urease affects the outcome of intracellular pathogenesis by modulating phagolysosomal pH. *PLoS Pathog* **2018**, *14*, e1007144, doi:10.1371/journal.ppat.1007144.

13. De Leon-Rodriguez, C.M.; Fu, M.S.; Çorbali, M.O.; Cordero, R.J.B.; Casadevall, A. The Capsule of Cryptococcus neoformans Modulates Phagosomal pH through Its Acid-Base Properties. *mSphere* **2018**, *3*, doi:10.1128/mSphere.00437-18.
14. Altamirano, S.; Li, Z.; Fu, M.S.; Ding, M.; Fulton, S.R.; Yoder, J.M.; Tran, V.; Nielsen, K. The Cyclin Cln1 Controls Polyploid Titan Cell Formation following a Stress-Induced G(2) Arrest in Cryptococcus. *mBio* **2021**, *12*, e0250921, doi:10.1128/mBio.02509-21.
15. Santiago-Burgos, E.J.; Stuckey, P.V.; Santiago-Tirado, F.H. Real-time visualization of phagosomal pH manipulation by Cryptococcus neoformans in an immune signal-dependent way. *Front Cell Infect Microbiol* **2022**, *12*, 967486, doi:10.3389/fcimb.2022.967486.
16. Roberts, G.D.; Horstmeier, C.D.; Land, G.A.; Foxworth, J.H. Rapid urea broth test for yeasts. *J Clin Microbiol* **1978**, *7*, 584-588, doi:10.1128/jcm.7.6.584-588.1978.
17. Feder, M.J.; Akyel, A.; Morasko, V.J.; Gerlach, R.; Phillips, A.J. Temperature-dependent inactivation and catalysis rates of plant-based ureases for engineered biomineralization. *Engineering Reports* **2021**, *3*, e12299, doi:https://doi.org/10.1002/eng2.12299.
18. Casadevall, A.; Cleare, W.; Feldmesser, M.; Glatman-Freedman, A.; Goldman, D.L.; Kozel, T.R.; Lendvai, N.; Mukherjee, J.; Pirofski, L.A.; Rivera, J.; et al. Characterization of a murine monoclonal antibody to Cryptococcus neoformans polysaccharide that is a candidate for human therapeutic studies. *Antimicrob Agents Chemother* **1998**, *42*, 1437-1446, doi:10.1128/aac.42.6.1437.
19. Rodrigues, J.; Ramos, C.L.; Frases, S.; Godinho, R.M.d.C.; Fonseca, F.L.; Rodrigues, M.L. Lack of chitin synthase genes impacts capsular architecture and cellular physiology in Cryptococcus neoformans. *The Cell Surface* **2018**, *2*, 14-23, doi:https://doi.org/10.1016/j.tcsw.2018.05.002.
20. Todd, R.T.; Braverman, A.L.; Selmecki, A. Flow Cytometry Analysis of Fungal Ploidy. *Current Protocols in Microbiology* **2018**, *50*, e58, doi:https://doi.org/10.1002/cpmc.58.
21. Samantaray, S.; Correia, J.N.; Garelnabi, M.; Voelz, K.; May, R.C.; Hall, R.A. Novel cell-based in vitro screen to identify small-molecule inhibitors against intracellular replication of Cryptococcus neoformans in macrophages. *Int J Antimicrob Agents* **2016**, *48*, 69-77, doi:10.1016/j.ijantimicag.2016.04.018.
22. Jamil, K.; Polyak, M.J.; Feehan, D.D.; Surmanowicz, P.; Stack, D.; Li, S.S.; Ogbomo, H.; Olszewski, M.; Ganguly, A.; Mody, C.H. Phagosomal F-Actin Retention by Cryptococcus gattii Induces Dendritic Cell Immunoparalysis. *mBio* **2020**, *11*, doi:10.1128/mBio.01821-20.
23. Yoneda, A.; Doering, T.L. A eukaryotic capsular polysaccharide is synthesized intracellularly and secreted via exocytosis. *Mol Biol Cell* **2006**, *17*, 5131-5140, doi:10.1091/mbc.e06-08-0701.
24. García-Rodas, R.; Cordero, R.J.; Trevijano-Contador, N.; Janbon, G.; Moyrand, F.; Casadevall, A.; Zaragoza, O. Capsule growth in Cryptococcus neoformans is coordinated with cell cycle progression. *mBio* **2014**, *5*, e00945-00914, doi:10.1128/mBio.00945-14.
25. Stukes, S.; Casadevall, A. Visualizing non-lytic exocytosis of Cryptococcus neoformans from macrophages using digital light microscopy. *J Vis Exp* **2014**, e52084, doi:10.3791/52084.
26. Dragotakes, Q.; Jacobs, E.; Ramirez, L.S.; Yoon, O.I.; Perez-Stable, C.; Eden, H.; Pagnotta, J.; Vij, R.; Bergman, A.; D'Alessio, F.; et al. Bet-hedging antimicrobial strategies in macrophage phagosome acidification drive the dynamics of Cryptococcus neoformans intracellular escape mechanisms. *PLOS Pathogens* **2022**, *18*, e1010697, doi:10.1371/journal.ppat.1010697.
27. Dragotakes, Q.; Stouffer, K.M.; Fu, M.S.; Sella, Y.; Youn, C.; Yoon, O.I.; De Leon-Rodriguez, C.M.; Freij, J.B.; Bergman, A.; Casadevall, A. Macrophages use a bet-hedging strategy for antimicrobial activity in phagolysosomal acidification. *The Journal of Clinical Investigation* **2020**, *130*, 3805-3819, doi:10.1172/JCI133938.
28. Davis, M.J.; Eastman, A.J.; Qiu, Y.; Gregorka, B.; Kozel, T.R.; Osterholzer, J.J.; Curtis, J.L.; Swanson, J.A.; Olszewski, M.A. Cryptococcus neoformans-induced macrophage lysosome damage crucially contributes to fungal virulence. *J Immunol* **2015**, *194*, 2219-2231, doi:10.4049/jimmunol.1402376.
29. Gaylord, E.A.; Choy, H.L.; Doering, T.L. Dangerous Liaisons: Interactions of Cryptococcus neoformans with Host Phagocytes. *Pathogens* **2020**, *9*, 891.
30. Artavanis-Tsakonas, K.; Love, J.C.; Ploegh, H.L.; Vyas, J.M. Recruitment of CD63 to Cryptococcus neoformans phagosomes requires acidification. *Proceedings of the National Academy of Sciences* **2006**, *103*, 15945-15950, doi:doi:10.1073/pnas.0607528103.
31. Baker, R.P.; Casadevall, A. Reciprocal modulation of ammonia and melanin production has implications for cryptococcal virulence. *Nat Commun* **2023**, *14*, 849, doi:10.1038/s41467-023-36552-7.

 doi:10.20944/preprints202403.0330.v1

32. Orner, E.P.; Bhattacharya, S.; Kalenja, K.; Hayden, D.; Del Poeta, M.; Fries, B.C. Cell Wall-Associated Virulence Factors Contribute to Increased Resilience of Old Cryptococcus neoformans Cells. *Front Microbiol* **2019**, *10*, 2513, doi:10.3389/fmicb.2019.02513.
33. Bouklas, T.; Jain, N.; Fries, B.C. Modulation of Replicative Lifespan in Cryptococcus neoformans: Implications for Virulence. *Frontiers in Microbiology* **2017**, *8*, doi:10.3389/fmicb.2017.00098.
34. Weber, S.M.; Levitz, S.M. Chloroquine antagonizes the proinflammatory cytokine response to opportunistic fungi by alkalizing the fungal phagolysosome. *J Infect Dis* **2001**, *183*, 935-942, doi:10.1086/319259.
35. Tucker, S.C.; Casadevall, A. Replication of Cryptococcus neoformans in macrophages is accompanied by phagosomal permeabilization and accumulation of vesicles containing polysaccharide in the cytoplasm. *Proc Natl Acad Sci U S A* **2002**, *99*, 3165-3170, doi:10.1073/pnas.052702799.
36. Fu, J.; Morris, I.R.; Wickes, B.L. The Production of Monokaryotic Hyphae by Cryptococcus neoformans Can Be Induced by High Temperature Arrest of the Cell Cycle and Is Independent of Same-Sex Mating. *PLOS Pathogens* **2013**, *9*, e1003335, doi:10.1371/journal.ppat.1003335.
37. Harrison, B.D.; Hashemi, J.; Bibi, M.; Pulver, R.; Bavli, D.; Nahmias, Y.; Wellington, M.; Sapiro, G.; Berman, J. A tetraploid intermediate precedes aneuploid formation in yeasts exposed to fluconazole. *PLoS Biol* **2014**, *12*, e1001815, doi:10.1371/journal.pbio.1001815.
38. Cruz-Acuña, M.; Pacifici, N.; Lewis, J.S. Vomocytosis: Too Much Booze, Base, or Calcium? *mBio* **2019**, *10*, doi:10.1128/mBio.02526-19.